




Different patterns of association between white matter microstructure and plasma unsaturated fatty acids in those with high risk for psychosis and healthy participants

Wenjun Su,¹ Zhixing Li,¹ Lihua Xu ¹, Jiahui Zeng,¹ Yingying Tang,¹ Xiaochen Tang,¹ Yanyan Wei ¹, Qian Guo,¹ Tianhong Zhang ¹, Jijun Wang^{1,2,3}

To cite: Su W, Li Z, Xu L, *et al.* Different patterns of association between white matter microstructure and plasma unsaturated fatty acids in those with high risk for psychosis and healthy participants. *General Psychiatry* 2022;**35**:e100703. doi:10.1136/gpsych-2021-100703

► Additional supplemental material is published online only. To view, please visit the journal online (<http://dx.doi.org/10.1136/gpsych-2021-100703>).

WS and ZL contributed equally.

Received 06 December 2021

Accepted 07 March 2022



© Author(s) (or their employer(s)) 2022. Re-use permitted under CC BY-NC. No commercial re-use. See rights and permissions. Published by BMJ.

For numbered affiliations see end of article.

Correspondence to

Dr Jijun Wang;
jijunwang27@163.com

Dr Tianhong Zhang;
zhang_tianhong@126.com

Dr Qian Guo;
alice4ever1205@126.com

ABSTRACT

Background Disrupted white matter (WM) microstructure has been commonly identified in youth at clinical high risk (CHR) for psychosis. Several lines of evidence suggest that fatty acids, especially unsaturated fatty acids (UFAs), might play a crucial role in the WM pathology of early onset psychosis. However, evidence linking UFA and WM microstructure in CHR is quite sparse.

Aims We investigated the relationship between the plasma UFA level and WM microstructure in CHR participants and healthy controls (HC).

Methods Plasma fatty acids were assessed and diffusion tensor imaging (DTI) data were performed with tract-based spatial statistics (TBSS) analysis for 66 individuals at CHR for psychosis and 70 HC.

Results Both the global and regional diffusion measures showed significant between-group differences, with decreased fractional anisotropy (FA) but increased mean diffusivity (MD) and radial diffusivity (RD) found in the CHR group compared with the HC group. On top of that, we found that in the HC group, plasma arachidic acid showed obvious trend-level associations with higher global FA, lower global MD and lower global RD, which regionally spread over the corpus callosum, right anterior and superior corona radiata, bilateral anterior and posterior limb of the internal capsule, and bilateral superior longitudinal fasciculus. However, there were no associations between global WM measures and any UFA in the CHR group. Conversely, we even found negative associations between arachidic acid levels and regional FA values in the right superior longitudinal fasciculus and right retrolenticular part of the internal capsule in the CHR group.

Conclusions Compared with the HC group, CHR subjects exhibited a different pattern of association between WM microstructure and plasma UFA, with a neuroprotective effect found in the HC group but not in the CHR group. Such discrepancy could be due to the excessively upregulated UFAs accumulated in the plasma of the CHR group, highlighting the role of balanced plasma-membrane fatty acids homeostasis in WM development.

INTRODUCTION

White matter (WM) pathological changes have been highlighted in the pathophysiology

Key messages

What is already known on this topic?

► Disrupted white matter (WM) microstructure has been commonly identified in youth at clinical high risk (CHR) for psychosis. Unsaturated fatty acid (UFA) might play a crucial role in the WM pathology and development. However, there is sparse evidence directly linking the UFA level and WM microstructure in CHR.

What this study adds?

► This study found different patterns of association between WM microstructure and plasma UFA level in CHR and HC. A neuroprotective effect of UFA was identified in the HC but not in the CHR.

How this study might affect research, practice or policy?

► Our findings highlighted the role of balanced plasma-membrane fatty acids homeostasis in normal WM development and myelination, provided new neuroimaging evidence for the pathophysiological relevance and future intervention of fatty acids in CHR.

of schizophrenia (SZ).¹ Cumulative evidence led to the demyelination and dysconnectivity hypothesis—that the dysfunctional oligodendrocytes which produce and maintain myelin within the central nervous system could underlie the abnormal or inefficient communication between neural cells, and to a larger extent, between distant functional brain regions, and thus increase psychotic symptoms such as hallucinations and thought disorders, or neurocognitive deficits in SZ.^{2,3} WM microstructure could be confounded by a series of intertwined effects such as cumulative antipsychotic exposure, neuroinflammation, and metabolism changes increased by medication, normal neurodegeneration,

and the progression of psychosis. Thus, studies of individuals at clinical high risk (CHR) for developing psychosis are greatly needed, as they have the advantage of being able to observe the origins of WM pathology, thereby shedding light on the underlying mechanisms prior to the onset of psychosis. Disrupted WM microstructure has been reported by many studies in CHR subjects, particularly in the corpus callosum (CC), superior and inferior longitudinal fasciculus, inferior frontal-occipital fasciculus, posterior and anterior limb of thalamic radiations, cingulum bundle, and uncinate fasciculus,⁴ suggesting a widespread pre-existing neurodevelopmental abnormality ahead of the first psychosis onset. Furthermore, the peak onset of SZ falls between 15 and 25 years of age, which is the developmental period of major brain WM tracts responsible for higher-order cognitive function, making individuals in this age group particularly vulnerable to the onset of psychopathology.⁵ Research has pinpointed that deficits in the long-range association tracts in CHR subjects are due to the blunting of expected age-related increases in WM volume and integrity,⁵ indicating that WM development could underlie the crucial pathophysiology in psychosis.

Myelin sheaths in the central nervous system comprise the lipid membranes of oligodendrocytes, and the membranes mainly consist of unsaturated fatty acids (UFAs).⁶ The amount of polyunsaturated fatty acids (PUFAs) intake could influence the rate of phospholipid synthesis and the energy supply, which affects the quantity and quality of membrane phospholipids, and in turn, causes amyelination, demyelination, and abnormal development of WM, leading to a susceptibility to psychosis.⁷ For example, Schwarz *et al* reported significantly altered free fatty acids (FFA) in both the grey and WM of patients with SZ.⁸ Furthermore, there is also evidence showing that PUFA supplementation could stimulate the expression of myelin proteins in rat brains, and slow down the cortical thickness reduction in parieto-occipital regions in patients with first-episode schizophrenia,⁹ indicating a neuroprotective effect of PUFA. Emerging studies also investigated whether omega-3 PUFA supplementation could ameliorate psychotic symptoms or global function and reduce the conversion rate to psychosis in CHR subjects.¹⁰ Considering that active WM myelination during adolescence and young adulthood may require more vigorous consumption of fatty acids, it is plausible that the fatty acids concentration, especially the UFA, might play a crucial role in the WM pathology underpinning in early onset psychosis.

A large body of evidence identified altered fatty acids in patients with psychosis. For example, a targeted metabolomics study reported significantly increased serum UFA in patients with SZ,¹¹ while another study identified multiple UFA and ketone bodies in both the serum and urine of patients with SZ,¹² suggesting an upregulated fatty acid catabolism. However, studies in CHR have not been fruitful so far. Our recent study found that among all of the pathways showing significant group differences,

the most perturbed (upregulated) pathway was involved in the biosynthesis of UFAs, with 11 significant FFAs being identified in the CHR subjects.¹³ The drastically altered fatty acids could impact neuron function through two main mechanisms: (1) membrane regeneration and neurotransmission: fatty acids modulate the activity of membrane transporters, receptors, ion channels, and enzymes. Furthermore, the decomposer of PUFA also could work as second messengers in intercellular and intracellular signal transductions¹⁴; (2) inflammation: after being released from the cell membrane, PUFA could be transformed into different pro-inflammatory and anti-inflammatory factors. Thus, the increased lipids metabolism could cause altered immune function, and in turn, lead to the inflammatory changes in WM, which is reflected as altered free-water (FW) in diffusion magnetic resonance imaging (dMRI) studies of SZ.¹⁵⁻¹⁶ Therefore, it is of great importance to investigate the effect of identified perturbed fatty acids on WM dysconnectivity, providing further reinforcement to the established link between fatty acids and WM in SZ pathophysiology.

However, there is sparse evidence directly linking fatty acid levels and WM microstructure in psychosis. Currently, only two studies have investigated the effect of fatty acid levels on WM in SZ. One study of 12 male patients with recent-onset SZ reported a significant positive correlation between total PUFA concentration in erythrocyte membranes and fractional anisotropy (FA) in bilateral uncinate fasciculus.¹⁷ Another study of 30 male patients with recent-onset SZ also reported a positive association between PUFA levels in erythrocyte membranes and FA, but in a quite large region, including the CC, bilateral parietal, occipital, temporal, and frontal WM.⁶ Such results are in line with the results of animal-level research, indicating that UFA could be responsible for the demyelination in SZ. However, these two studies did not include female patients and lacked healthy controls (HC). Whether the altered UFA level could affect WM demyelination prior to the psychosis onset, and whether it could influence the severity of psychotic symptoms through the mediation of WM, have not yet been documented.

In the present study, we aimed to investigate the relationship between the plasma UFA level and WM microstructure in individuals with CHR of psychosis and healthy participants. We hypothesised that the 11 preidentified plasma UFAs would be associated with WM microstructure. As an additional analysis, we also explored the association between UFA-related WM microstructural abnormalities and psychotic symptoms of CHR participants.

METHODS

Participants

The process of sample selection is illustrated in [figure 1](#). Participants were recruited at the Shanghai Mental Health Center (SMHC) as a part of the Shanghai At-Risk for Psychosis Extending Programme.¹⁸ All patients were medication-naïve and fulfilled the diagnostic criteria for

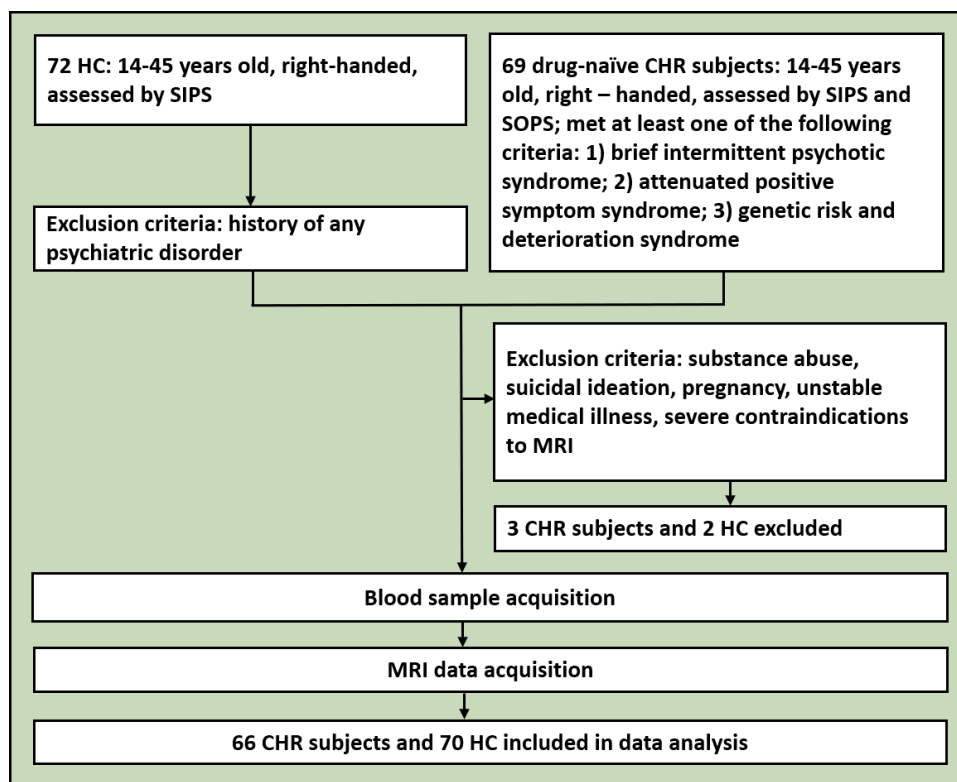


Figure 1 Flowchart of sample selection. CHR, clinical high risk; HC, healthy controls; MRI, magnetic resonance imaging; SIPS, Structured Interview for Prodromal Syndromes; SOPS, Scale of Prodromal Symptoms.

CHR for psychosis based on the Chinese version of the Structured Interview for Prodromal Syndromes (SIPS) and the Scale of Prodromal Symptoms (SOPS) as identified by a senior psychiatrist.¹⁹ Individuals had to fulfil at least one of the following criteria to meet the diagnosis of CHR: (1) brief intermittent psychotic syndrome, (2) attenuated positive symptom syndrome or (3) genetic risk and deterioration syndrome. The current Global Assessment of Functioning Scale (GAF) and GAF scores drop (relative to 12 months prior) were assessed to evaluate the functional deterioration of CHR group participants.²⁰ HCs were recruited via online advertisement and were assessed using SIPS to exclude a history of clinical high-risk syndrome, and the non-patient version of Structured Clinical Interview for Diagnostic and Statistical Manual of Mental Disorders, Fourth Edition to exclude a history of any psychiatric disorder. Participants were between the ages of 14 and 45 years; were right-handed; were free of substance abuse, suicidal ideation, pregnancy, unstable medical illness and had no severe contraindications to MRI. Three CHR participants and two healthy participants were excluded because of their physical conditions. Finally, 66 drug-naïve CHR individuals and 70 HC were included in the statistical analysis.

Image acquisition

MRI scans were acquired on a 3.0 T Siemens MR B17 (Verio) system with 32-channel head coil at SMHC. Prior to scanning, foam padding was placed around the participant's head to avoid gross head motion. Three-dimensional

structural images were acquired using a T1-weighted magnetization-prepared rapid gradient echo (MPRAGE) sequence with repetition time (TR)=2300 ms, echo time (TE)=2.96 ms, field of view (FOV)=256 mm, voxel size=1.0 mm×1.0 mm×1.0 mm, 192 contiguous sagittal slices, slice thickness=1 mm, acquisition matrix=256×256 and acquisition time (TA)=9'14". Multishell dMRI data were acquired by 30 gradient directions at $b=3000\text{ s/mm}^2$, 30 at $b=1000\text{ s/mm}^2$, 6 at $b=500\text{ s/mm}^2$, 3 at $b=200\text{ s/mm}^2$ and 5 interleaved b_0 images; with TR=15 800 ms, TE=109 ms, FOV=256 mm, voxel size=2.0×2.0×2.0 mm³, 70 transversal slices, slice thickness=2 mm, resolution matrix size=128×128 and TA=20'17".

Image processing

Image processing was conducted with tools from the FSL V.5.0.9 (FMRIB Software Library, <http://www.fmrib.ox.ac.uk/fsl>).^{21 22} Diffusion images were axis-aligned, centred and visually inspected slice-by-slice by an experienced researcher before preprocessing to exclude severe image artefacts (eg, multiple dropped signals, gross head motion or ghosting). All diffusion images passed the quality control measures. Images were first corrected for eddy currents and head motion using the linear image registration tool (FLIRT V.6.0). Subsequently, the individual brain masks were generated based on the b_0 image using the brain-extraction tool (V.2.1). Finally, FMRIB's diffusion toolbox (V.3.0) was used to calculate eigenvalues λ_1 , λ_2 , λ_3 and generate individual FA, radial diffusivity (RD), and mean diffusivity (MD) maps. Before

calculation, we omitted gradient directions other than b value at 0 and 1000 in order to circumvent non-Gaussian effects.

A voxel-wise statistical analysis was carried out using tract-based spatial statistics (TBSS) analysis (<https://fsl.fmrib.ox.ac.uk/fsl/fslwiki/TBSS>) in FSL.^{21, 22} For the next step, all the FA images were aligned into 1 mm×1 mm×1 mm Montreal Neurological Institute 152 space using the FMRIB's Non-linear Image Registration Tool implemented in FSL. Next, the mean FA image was created and thinned to generate a mean FA skeleton, which represents the centres of all tracts common to the group, with a threshold of 0.2 to keep only the main tracts. Each subject's FA, MD and RD data were then projected onto the skeleton, and the resulting data were fed into voxel-wise cross-individual statistics.

Unsaturated fatty acids

The procedures of sample collection, preparation and the UPLC-Q-TOF/MS data acquisition are described in detail in our previous study.¹³ Briefly, venous blood samples were collected at the Shanghai Mental Health Center from individuals after overnight fasting. Plasma samples were separated instantly and stored at -80°C until the ultra performance liquid chromatography coupled with quadrupole time-of-flight mass spectrometry (UPLC-Q-TOF/MS) analysis. The metabolites were identified by accuracy mass (<25 ppm) and secondary mass spectrometry data by matching with a standard database. The Kyoto Encyclopedia of Genes and Genomes (KEGG) pathway analysis was performed to identify the perturbed pathways and the metabolites that differed CHR from HC. The fatty acids involved in this study were selected from the most perturbed pathway 'biosynthesis of UFAs' in our previous case-control sample, which contains 11 different metabolites: (4Z,7Z,10Z,13Z,16Z,19Z)-4,7,10,13,16,19-docosahexaenoic acid (DHA); arachidonic acid (ARA); arachidic acid (AA); nervonic acid (NA); palmitic acid (PA); behenic acid (BA); stearic acid (SA); oleic acid (OA); tetracosanoic acid (TA); erucic acid (EA) and linoleic acid (LA).

Statistical analysis

The workflow of statistical analysis performed in our study is illustrated in [figure 1](#). Statistical analyses were conducted using R V.4.0.5. Two independent sample t-tests were used to examine the differences of age, while χ^2 tests were performed to examine the differences of sex between the two groups. Considering that most of the UFAs were not normally distributed, Mann-Whitney U tests were performed to examine the between-group differences of the 11 UFAs. Next, UFAs that showed significant between-group differences were considered as UFAs of interest and fed into further analysis with dMRI measures. The results were shown as mean (SD) with significant difference considered at $p < 0.05$.

Two independent samples t-tests were performed to detect the between-group differences in FA, MD and RD

using the FSL randomisation programme (5000 permutations) implemented in FSL, with age and sex controlled as covariates. Statistical thresholds were set at a p value of 0.05, with familywise error corrected and threshold-free cluster enhancement corrected. The Johns Hopkins University diffusion tensor imaging (DTI)-based WM atlas in FSL toolbox (ICBM-DTI-81 atlas) was used to identify the localisation of abnormal WM fibre tracts. The mean FA, MD and RD values in the regions with significant case-control group differences were then extracted and further fed into R to perform further analysis.

We then tested the main hypothesis that the perturbed UFA level would be associated with WM microstructure. To reduce the burden of multiple testing, we undertook principal component analysis (PCA) to index the general WM impairment in CHR using R package 'psych' V.2.1.3. dMRI measures in the region that showed significant group differences were subjected to PCA analysis, for which the first unrotated principal component was derived, and termed three global dMRI measures: global FA (gFA), global MD (gMD), and global RD (gRD). Furthermore, post hoc t-tests were then performed to assure the power of global dMRI measures for differences between CHR and HC groups. Then we performed the Spearman's rank correlations to test the association between the global dMRI measures and the UFAs of interest separately in the CHR and HC groups. For the UFAs that showed significant association with global dMRI measures, further association tests were then performed for the regional dMRI measures to explore the spatial distribution of that UFA in the brain. As an additional analysis, we also explored the association between UFA-related WM abnormalities and clinical symptoms by Pearson's correlation tests. Results were considered statistically significant at $p < 0.05$.

RESULTS

Demographics, clinical characteristics and plasma UFAs levels

The demographics, clinical characteristics, and plasma UFA levels of both the CHR and HC groups are shown in [table 1](#). There were no significant differences in age ($t = 1.78$, $p = 0.084$) and sex ($\chi^2 = 0.21$, $p = 0.647$) between the CHR and HC groups. Plasma UFAs showed significant effect on distinguishing the CHR group from HC, with a tremendously lower DHA ($Z = -6.79$, $p < 0.001$), OA ($Z = -5.08$, $p < 0.001$), and LA ($Z = -6.71$, $p < 0.001$), but higher ARA ($Z = 10.03$, $p < 0.001$), AA ($Z = 8.81$, $p < 0.001$), BA ($Z = 9.46$, $p < 0.001$), EA ($Z = 4.90$, $p < 0.001$), NA ($Z = 5.09$, $p < 0.001$), PA ($Z = 8.67$, $p < 0.001$), SA ($Z = 8.67$, $p < 0.001$), and TA ($Z = 7.86$, $p < 0.001$) observed in the CHR group.

Widespread WM microstructural changes in CHR subjects

We first investigated the differences in mean FA, MD and RD between the CHR and HC groups. Compared with the HC group, CHR subjects showed significantly decreased FA but increased MD and RD, spreading over many regions, including the CC, bilateral corona radiata (CR), bilateral superior longitudinal fasciculus (SLF), bilateral

Table 1 Demographics, clinical characteristics and plasma unsaturated fatty acids levels

	CHR (n=66)	HC (n=70)	Statistics	P value
Age, mean (SD)	18.30 (4.19)	17.30 (2.10)	1.78	0.084*
Gender, male/female	38/28	43/27	0.21	0.647‡
DHA, mean (SD)	6.08 (4.15) E+04	1.41 (1.07) e+05	-6.79	<0.001†
ARA, mean (SD)	4.88 (1.56) E+04	1.20 (0.48) e+04	10.03	<0.001†
AA, mean (SD)	6.69 (1.47) E+04	3.71 (1.25) e+04	8.81	<0.001†
BA, mean (SD)	2.68 (0.88) E+04	1.01 (0.53) e+04	9.46	<0.001†
EA, mean (SD)	2.52 (6.20) E+04	1.10 (1.53) e+04	4.90	<0.001†
NA, mean (SD)	2.04 (1.39) E+04	1.24 (0.63) e+04	5.09	<0.001†
OA, mean (SD)	1.15 (0.50) E+05	2.68 (1.79) e+05	-5.08	<0.001†
PA, mean (SD)	7.65 (2.26) E+03	2.78 (2.04) e+03	8.67	<0.001†
SA, mean (SD)	5.57 (0.89) E+06	2.92 (1.39) e+06	8.67	<0.001†
TA, mean (SD)	1.43 (0.89) E+04	6.13 (3.63) e+03	7.86	<0.001†
LA, mean (SD)	3.63 (1.33) E+03	9.74 (8.91) e+03	-6.71	<0.001†
SOPS positive score, mean (SD)	10.33 (3.91)	-	-	-
SOPS negative score, mean (SD)	12.23 (6.72)	-	-	-
SOPS disorganisation score, mean (SD)	7.23 (3.71)	-	-	-
SOPS general score, mean (SD)	8.83 (2.84)	-	-	-
GAF current score	53.67 (9.47)	-	-	-
GAF drop in past 12 months	24.06 (8.25)	-	-	-

*Independent sample t-test.

†Mann-Whitney U test.

‡ χ^2 test.

AA, arachidic acid; ARA, arachidonic acid; BA, behenic acid; CHR, clinical high-risk psychosis; DHA, (4Z,7Z,10Z,13Z,16Z,19Z)-4,7,10,13,16,19-docosahexaenoic acid; EA, erucic acid; GAF, Global Assessment of Functioning Scale; HC, healthy control; LA, linoleic acid; NA, nervonic acid; OA, oleic acid; PA, palmitic acid; SA, stearic acid; SD, standard deviation; SOPS, Scale of Prodromal Symptoms; TA, tetracosanoic acid.

anterior limb of internal capsule (ALIC), bilateral posterior limb of internal capsule (PLIC), and the bilateral cerebral peduncle (CP) (figure 2A, online supplemental table S1). In terms of global microstructural measures, patients also showed significant decreased gFA but increased gMD and gRD (figure 2B), indicating a robust power of global dMRI measures for differentiating the CHR group from HC.

Association between WM microstructure and plasma UFAs levels

We then tested the association between perturbed UFAs and regional/global dMRI measures in the CHR and HC groups, respectively. Among all of the FFAs, only AA showed obvious trend-level associations in all of the global dMRI measures, with a positive association related to gFA, but a negative association with gMD and gRD in the HC group (figure 3A). However, there were no associations observed in the CHR group. Regional analysis found significantly positive associations between mean FA values and AA level in the HC group, including the left fornix (FX) ($r=0.29$, $p=0.017$), right FX ($r=0.25$, $p=0.036$), left posterior thalamic radiation ($r=0.26$, $p=0.027$), left anterior corona radiata (ACR) ($r=0.26$, $p=0.029$), right PLIC ($r=0.29$, $p=0.017$), and left ALIC ($r=0.24$, $p=0.049$).

In the HC group, plasma AA level was also negatively associated with the mean MD values in the left SLF ($r=-0.28$, $p=0.020$), right SLF ($r=-0.28$, $p=0.018$), right superior corona radiata (SCR) ($r=-0.27$, $p=0.022$), right ACR ($r=-0.28$, $p=0.019$), the splenium of CC ($r=-0.26$, $p=0.029$), and genu of CC ($r=-0.25$, $p=0.039$); and the mean RD values in the right sagittal stratum ($r=-0.24$, $p=0.049$), right ACR ($r=-0.26$, $p=0.032$), right SCR ($r=-0.29$, $p=0.016$), right PLIC ($r=-0.25$, $p=0.034$), left ALIC ($r=-0.27$, $p=0.024$), right ALIC ($r=-0.27$, $p=0.022$), body of CC ($r=-0.25$, $p=0.035$), and genu of CC ($r=-0.27$, $p=0.022$). However, in the CHR group, AA only showed negative associations with the mean FA value in the right SLF ($r=-0.26$, $p=0.038$) and right retrolenticular part of internal capsule (RLIC) ($r=-0.31$, $p=0.011$) and the mean RD value in the left inferior cerebellar peduncle (ICP) ($r=-0.30$, $p=0.014$) (figure 3B).

UFA, WM microstructure and clinical characteristics

We first tested the associations between global dMRI measures and clinical characteristics. The gMD showed significant negative association with GAF current scores ($r=-0.31$, $p=0.011$), but positive association with GAF score drop in the past 12 months ($r=0.29$, $p=0.017$) and SOPS negative score ($r=0.31$, $p=0.011$) (figure 4A).

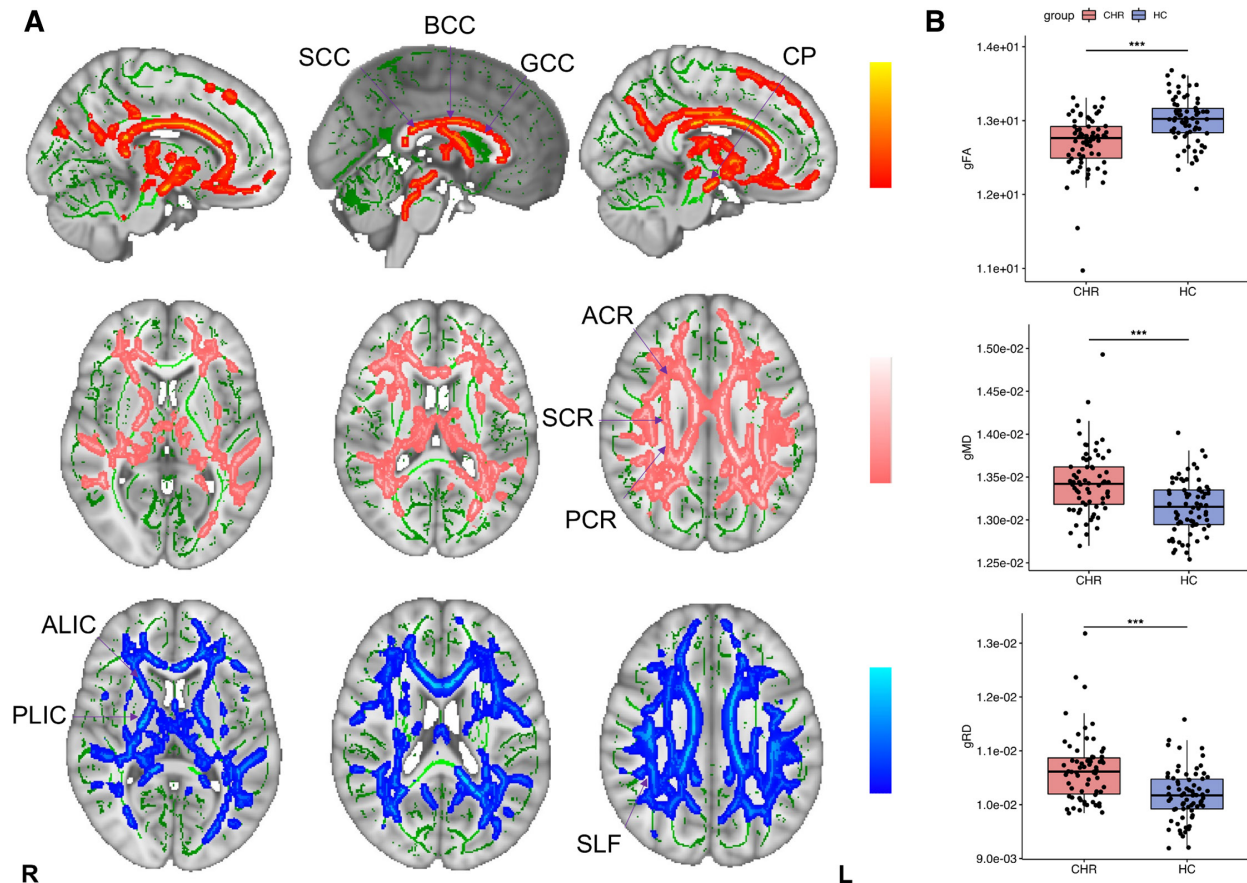


Figure 2 Group comparison for regional and global fractional anisotropy (FA), radial diffusivity (RD) and mean diffusivity (MD) in clinical high risk (CHR) group and healthy control (HC) group. (A) Tract-based spatial statistics analysis (TBSS) showed widespread significant between-group difference in regional microstructural diffusion magnetic resonance imaging (dMRI) measures, with significantly lower FA but higher MD and RD values found in the CHR group, compared with the HC group. Significant lower FA values (red), higher MD (pink) and higher RD (blue) are drawn on top of the white matter skeleton (green). Images are shown at a permutation-based threshold of $p < 0.05$ (family-wise error corrected). The colour bars represent the 1-p value (0.95–1). (B) Two independent samples t-tests of global FA (gFA), global MD (gMD) and global RD (gRD) between CHR and HC group. CHR showed significant decreased gFA, increased gMD and gRD compared with HC group. ACR, anterior corona radiata; ALIC, anterior limb of internal capsule; BCC, body of the corpus callosum; CP, cerebral peduncle; GCC, genu of the corpus callosum; PCR, posterior corona radiata; PLIC, posterior limb of internal capsule; SCC, splenium of the corpus callosum; SCR, superior corona radiata; SLF, superior longitudinal fasciculus. *** $p < 0.001$.

Likewise, gRD also showed significant negative association with GAF current scores ($r = -0.30$, $p = 0.016$) and positive association with GAF score drop in the past 12 months ($r = 0.33$, $p = 0.007$). The gRD was also marginally associated with SOPS negative score ($r = 0.23$, $p = 0.059$) (figure 4B). In terms of the UFA-related regional dMRI measures, FA in the right RLIC was positively correlated with the SOPS disorganisation score ($r = 0.27$, $p = 0.031$), while no associations were found in the SLF or ICP. In terms of UFA, plasma AA level showed no association with the SOPS scores, neither with the GAF scores nor with the GAF drop scores.

DISCUSSION

Main findings

In this study, we found decreased FA but increased MD and RD in many regions in CHR group participants compared with HC, including the CC, bilateral CR, bilateral SLF,

bilateral ALIC, bilateral PLIC, and bilateral CP. Global WM measures also showed significant between-group differences, with a decreased gFA but increased gMD and gRD found in the CHR group compared with the HC group. On top of that, our study for the first time reported that in the healthy participants, AA level showed an obvious trend-level association with higher gFA, lower gMD, and lower RD, which regionally spread over CC, right ACR and SCR, bilateral ALIC and PLIC, and bilateral SLF. However, there was no association between global WM measures and any UFA level in the CHR group. Conversely, we even found negative association between AA level and regional FA values in the right SLF and right RLIC in the CHR group. Thus, our results suggested that, compared with HC, CHR subjects showed different patterns of association between WM microstructure and plasma UFA level, with a neuroprotective effect found in the healthy participants but not in the CHR group participants.

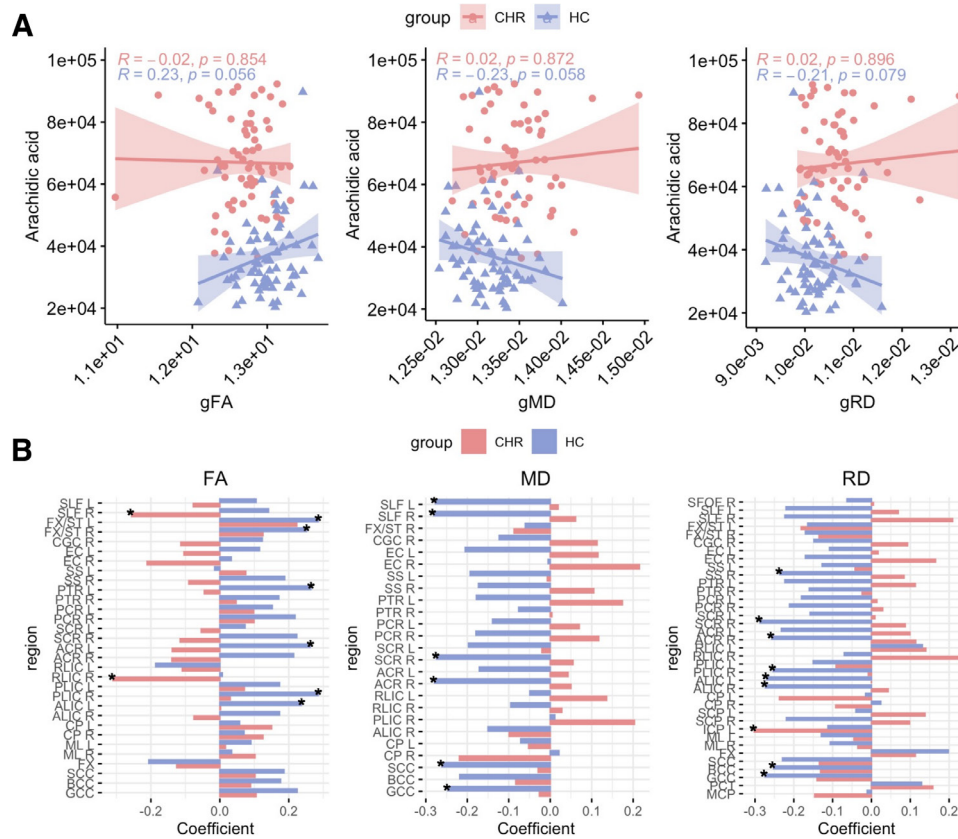


Figure 3 Association between plasma arachidic acid level and regional/global fractional anisotropy (FA), radial diffusivity (RD) and mean diffusivity (MD) in clinical high risk (CHR) group and healthy control (HC) group. (A) In the HC group, arachidic acid level showed obvious trend-level associations with all the global diffusion magnetic resonance imaging (dMRI) measures, with a positive association related to global FA (gFA), but a negative association with global MD (gMD) and global RD (gRD). (B) Association coefficients between arachidic acid level and regional FA, MD and RD values. ACR, anterior corona radiata; ALIC, anterior limb of internal capsule; BCC, body of the corpus callosum; CGC, cingulum; CP, cerebral peduncle; EC, external capsule; FX, fornix; FX/ST, fornix stria terminalis; GCC, genu of the corpus callosum; ICP, inferior cerebellar peduncle; MCP, middle cerebellar peduncle; ML, medial lemniscus; PCR, posterior corona radiata; PCT, pontine crossing tract; PLIC, posterior limb of internal capsule; PTR, posterior thalamic radiation; RLIC, retrolenticular part of internal capsule; SCR, splenium of the corpus callosum; SCP, superior cerebellar peduncle; SCR, superior corona radiata; SFOF, superior fronto-occipital fasciculus; SLF, superior longitudinal fasciculus; SS, sagittal stratum. * $p < 0.05$.

In line with a number of previous studies, our study reported a widespread microstructural disruption in the WM of CHR participants, mainly spreading over the CC, bilateral CR, bilateral SLF, bilateral ALIC and PLIC, and bilateral CP. Deficits in these WM regions have been commonly identified in many previous studies of CHR persons, which underlie more severe psychotic symptoms, poor functioning, and elevated conversion risks of CHR,^{4 23 24} indicating pre-existing myelination prior to the psychosis onset.

Similarly, the drastically upregulated plasma UFAs level was also identified in previous psychosis studies. Most of the evidence pointed to an elevated UFA level in plasma or serum,^{11 12} but a decreased UFA level in erythrocyte membranes in patients with SZ.^{25 26} One study of help-seeking CHR patients also reported decreased nervonic acid in erythrocyte membranes, which correlated with prodromal symptoms and predicted conversion to psychosis.²⁷ Although it is not fully elucidated yet, the majority of research posited that these opposite findings

in plasma and erythrocyte membranes stem from the ‘turnover’ mechanism: fatty acids are released from membrane to plasma and become FFAs, which could be transformed to fatty acids-CoA and further reincorporate to the membrane, replace the impaired fatty acids on the membrane, and thus, maintain the dynamic biological balance in oligodendrocytes and myelin.²⁸ A magnetic resonance spectroscopy (MRS) study in children and adolescents with CHR also reported decreased precursors and increased breakdown products of membrane phospholipid synthesis, suggesting a decreased incorporation of FFA and increased membrane catabolism presented in the early course of SZ.²⁹ Thus, the distinct pattern of association between WM microstructure and plasma AA levels in those at CHR and HC found in our study could be the reflection of imbalanced homeostasis between plasma FFA and membrane phospholipids. Specifically, AA has been identified as a prospective biomarker differentiating SZ from healthy populations.³⁰ In healthy participants, the plasma AA level was positively correlated with both

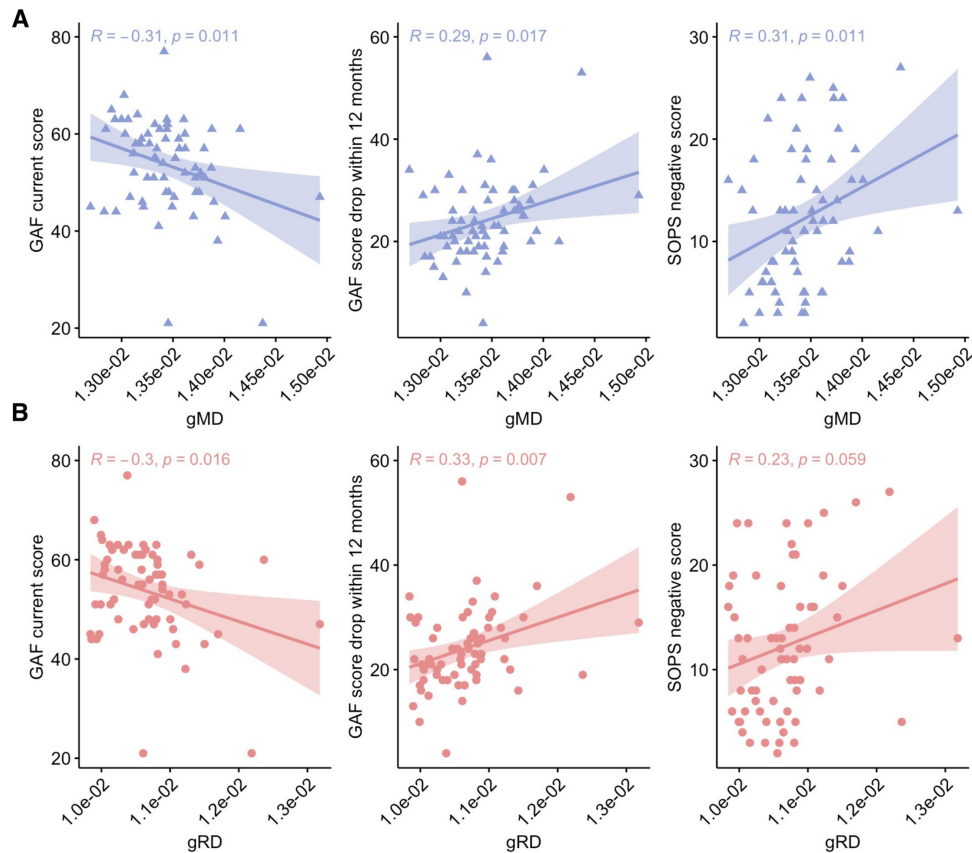


Figure 4 Association between clinical characteristics and global diffusion magnetic resonance imaging (dMRI) measures. (A) Global mean diffusivity (gMD) showed significant negative association with Global Assessment of Functioning Scale (GAF) current scores, but positive association with GAF scores drop in 12 months, and Scale of Prodromal Symptoms (SOPS) negative scores. (B) Global radial diffusivity (gRD) showed significant negative association with GAF current scores and positive association with GAF score drop in the past 12 months, and also showed a marginally positive association with SOPS negative scores.

regional and global FA values and negatively correlated with regional and global MD/RD values, indicating a neuroprotective effect for WM development and myelination. In contrast, there were no associations between global dMRI measures and any UFA, and even negative association between AA and mean FA values in the right SLF and RLIC. Therefore, it is reasonable to postulate that the homeostatic balance between membrane-plasma fatty acids could, to some extent, play the optimal neuroprotective function and promote WM development, while the excessively upregulated fatty acids accumulated in the plasma break this balance and work as an ‘inhibitor’ for normal myelination. This explanation is further reinforced by a study from McNamara *et al*, who reported a U-curve association between total UFA concentration and axial diffusivity in the inferior longitudinal fasciculus and between phospholipase A2 activity and average WM FA,³¹ lending credibility to our results. However, such explanation should be rendered with caution since we did not measure the membrane fatty acids altogether. Further research is required to characterise the association between membrane fatty acid and WM, addressing this hypothesis in greater detail.

We also investigated the association between plasma AA level, WM dysconnectivity and clinical characteristics in CHR group participants. Our results showed that in the CHR group, gMD showed significant negative association with GAF current scores, but positive association with GAF score drop in the past 12 months and SOPS negative scores. Likewise, gRD also showed significant negative association with GAF current scores and positive association with GAF score drop in the past 12 months. The gRD was also marginally associated with SOPS negative scores. Such results suggest that the abnormal myelination found in our study could underlie poorer functioning and faster functional drop, as well as more severe negative symptoms prior to the onset of psychosis. Largely in line with previous studies, it is recognised that negative symptoms are commonly presented at the premorbid phase of psychosis and are frequently associated with poorer functioning, more cognitive impairments, and worse long-term outcome, especially in youth at CHR of psychosis.³² Since negative symptoms have been conceptualised as the insufficient communication between brain regions, the disrupted myelin found in our CHR sample could underlie the insufficiency of information communication

and integration between hemispheres, which subsequently gives rise to negative symptoms. However, despite the effect on both global and regional diffusion measures, there were no associations between AA level and clinical characteristics. These results highlighted the advantage of the neuroimaging method as a biologically proximate approach that could capture the effect of pathophysiological changes more sensitively than the behavioural-level measures, disentangling the underlying biological mechanism of the clinical complexity of psychosis.

Limitations

The findings of our study have to be considered in light of the following limitations. First, our sample size is relatively small. Although we found significant associations between regional dMRI measures and plasma AA level in the HC group, the association between AA and global measures are only marginally significant. This could be due to the limited sample size of our study. Further studies with a larger sample size are required to validate our findings. Second, as mentioned before, we did not measure the membrane fatty acids altogether. It would be of interest for future studies to investigate the direct link between membrane fatty acids, plasma FFAs, and WM, addressing this hypothesis in greater detail. Third, the methodological limitations of TBSS should be considered. TBSS limits the analysis to the major fibre tracts; thus, the directional information might be abandoned during the skeletonization process. Moreover, although it could perfectly characterise WM integrity of CHR patients and differentiate them from healthy participants, other biophysical information such as extracellular water are not taken into consideration. Further research using other diffusion methodology such as neurite orientation dispersion and density imaging and FW imaging are needed to illustrate other characteristics of WM at the imaging level, yielding more information such as inflammation and oxidation, which have been commonly identified in the biosynthesis mechanism of fatty acids.

Implications

Our study for the first time reported a distinct pattern of association between WM microstructure and plasma arachidic acid level in patients with clinical high-risk psychosis and healthy participants. Arachidic acid showed a significant neuroprotective effect for WM development and myelination, mainly spreading over the CC, right anterior and superior CR, bilateral ALIC and PLIC, and bilateral SLF. However, such effects were not found in the CHR group. Such discrepancy could be due to the excessively upregulated fatty acids accumulated in the plasma of CHR patients, highlighting the role of balanced plasma-membrane fatty acids homeostasis on normal myelination and WM development. Our study thus adds new neuroimaging evidence for the pathophysiological relevance of fatty acids and introduces a prominent new insight into the pathogenesis of SZ.

Author affiliations

¹Shanghai Key Laboratory of Psychotic Disorders, Shanghai Mental Health Center, Shanghai Jiao Tong University School of Medicine, Shanghai, China
²CAS Center for Excellence in Brain Science and Intelligence Technology (CEBSIT), Chinese Academy of Science, Shanghai, China
³Institute of Psychology and Behavioral Science, Shanghai Jiao Tong University, Shanghai, China

Acknowledgements We are grateful to the patients, their families and the healthy subjects who gave their time to participate in this study.

Contributors WS: contributed to the neuroimaging data analysis and writing of the manuscript. ZL: contributed to the metabolomics data analysis and data organisation. LX, JZ, YT, XT and YW: contributed to the recruitment, clinical assessment and data acquisition. QG, TZ and JW designed the study, provided supervision for the implementation of the study and the interpretation of the results. JW accepted full responsibility for the work and the conduct of the study, had access to the data, and controlled the decision to publish. All authors have contributed to and approved the final manuscript.

Funding This research was supported by National Natural Science Foundation of China grants (81971251, 81671329, 81871050, 82171497, 82101582, 82001406); Clinical Research Center at Shanghai Mental Health Center grants (CRC2018ZD01, CRC2018ZD04, CRC2018YB01, CRC2019ZD02); Clinical Research Center at Shanghai Jiao Tong University School of Medicine (DLY201817, 20190102); Shanghai Science and Technology Committee Foundations (19411950800, 16ZR1430500, 19411969100, 19410710800, 21ZR1481500, 20ZR1448600, 21S31903100, 19ZR14451); Shanghai Clinical Research Center for Mental Health (19MC1911100); Project of the Key Discipline Construction, Shanghai 3-Year Public Health Action Plan (GWV-10.1-XK18); Shanghai Municipal Science and Technology Major Project (2018SHZDZX01, 2018SHZDZX05) and ZJ Lab; Foundation of Shanghai Mental Health Center (2020-FX-02); Excellent Talents Training Project of Shanghai Municipal Commission of Health (GWV-10.2-YQ44).

Disclaimer These funding agents had no role in the study design, collection, analysis, and interpretation of the data, writing of the manuscript or decision to submit the paper for publication.

Competing interests None declared.

Patient consent for publication Not applicable.

Ethics approval This study was approved by the Research Ethics Committee of the SMHC (No. 2020-100). All participants or their legal guardians (for those younger than 18 years old) signed an informed consent document prior to study participation.

Provenance and peer review Commissioned; externally peer reviewed.

Data availability statement Data are available on reasonable request. The data used in this study are available from the corresponding author on reasonable request.

Supplemental material This content has been supplied by the author(s). It has not been vetted by BMJ Publishing Group Limited (BMJ) and may not have been peer-reviewed. Any opinions or recommendations discussed are solely those of the author(s) and are not endorsed by BMJ. BMJ disclaims all liability and responsibility arising from any reliance placed on the content. Where the content includes any translated material, BMJ does not warrant the accuracy and reliability of the translations (including but not limited to local regulations, clinical guidelines, terminology, drug names and drug dosages), and is not responsible for any error and/or omissions arising from translation and adaptation or otherwise.

Open access This is an open access article distributed in accordance with the Creative Commons Attribution Non Commercial (CC BY-NC 4.0) license, which permits others to distribute, remix, adapt, build upon this work non-commercially, and license their derivative works on different terms, provided the original work is properly cited, appropriate credit is given, any changes made indicated, and the use is non-commercial. See: <http://creativecommons.org/licenses/by-nc/4.0/>.

ORCID iDs

Lihua Xu <http://orcid.org/0000-0002-2237-9336>
 Yanyan Wei <http://orcid.org/0000-0002-8218-1954>
 Tianhong Zhang <http://orcid.org/0000-0002-5379-7119>

REFERENCES

- 1 Peters BD, Karlsgodt KH. White matter development in the early stages of psychosis. *Schizophr Res* 2015;161:61–9.
- 2 Ellison-Wright I, Bullmore E. Meta-analysis of diffusion tensor imaging studies in schizophrenia. *Schizophr Res* 2009;108:3–10.
- 3 Zhang H, Wang Y, Hu Y, et al. Meta-analysis of cognitive function in Chinese first-episode schizophrenia: MATRICS consensus cognitive battery (MCCB) profile of impairment. *Gen Psychiatr* 2019;32:e100043.
- 4 Waszczuk K, Rek-Owodziń K, Tyburski E, et al. Disturbances in white matter integrity in the ultra-high-risk psychosis state—a systematic review. *J Clin Med* 2021;10. doi:10.3390/jcm10112515. [Epub ahead of print: 06 06 2021].
- 5 Patel PK, Leathem LD, Currin DL, et al. Adolescent neurodevelopment and vulnerability to psychosis. *Biol Psychiatry* 2021;89:184–93.
- 6 Peters BD, Machielsen MWJ, Hoen WP, et al. Polyunsaturated fatty acid concentration predicts myelin integrity in early-phase psychosis. *Schizophr Bull* 2013;39:830–8.
- 7 Karlsgodt KH, Jacobson SC, Seal M, et al. The relationship of developmental changes in white matter to the onset of psychosis. *Curr Pharm Des* 2012;18:422–33.
- 8 Schwarz E, Prabhakaran S, Whitfield P, et al. High throughput lipidomic profiling of schizophrenia and bipolar disorder brain tissue reveals alterations of free fatty acids, phosphatidylcholines, and ceramides. *J Proteome Res* 2008;7:4266–77.
- 9 Pawelczyk T, Piątkowska-Janko E, Bogorodzki P, et al. Omega-3 fatty acid supplementation may prevent loss of gray matter thickness in the left parieto-occipital cortex in first episode schizophrenia: a secondary outcome analysis of the offer randomized controlled study. *Schizophr Res* 2018;195:168–75.
- 10 Hsu M-C, Huang Y-S, Ouyang W-C. Beneficial effects of omega-3 fatty acid supplementation in schizophrenia: possible mechanisms. *Lipids Health Dis* 2020;19:159.
- 11 Yang X, Sun L, Zhao A, et al. Serum fatty acid patterns in patients with schizophrenia: a targeted metabolomics study. *Transl Psychiatry* 2017;7:e1176.
- 12 Yang J, Chen T, Sun L, et al. Potential metabolite markers of schizophrenia. *Mol Psychiatry* 2013;18:67–78.
- 13 Li Z, Zhang T, Xu L, et al. Plasma metabolic alterations and potential biomarkers in individuals at clinical high risk for psychosis. *Schizophr Res* 2022;239:19–28.
- 14 Vijayakumar N, Bartholomeusz C, Whitford T, et al. White matter integrity in individuals at ultra-high risk for psychosis: a systematic review and discussion of the role of polyunsaturated fatty acids. *BMC Psychiatry* 2016;16:287.
- 15 Lyall AE, Pasternak O, Robinson DG, et al. Greater extracellular free-water in first-episode psychosis predicts better neurocognitive functioning. *Mol Psychiatry* 2018;23:701–7.
- 16 Guo JY, Lesh TA, Niendam TA, et al. Brain free water alterations in first-episode psychosis: a longitudinal analysis of diagnosis, course of illness, and medication effects. *Psychol Med* 2021;51:1001–10.
- 17 Peters BD, Duran M, Vlieger EJ, et al. Polyunsaturated fatty acids and brain white matter anisotropy in recent-onset schizophrenia: a preliminary study. *Prostaglandins Leukot Essent Fatty Acids* 2009;81:61–3.
- 18 Zhang T, Li H, Tang Y, et al. Validating the predictive accuracy of the NAPLS-2 psychosis risk calculator in a clinical high-risk sample from the sharp (Shanghai at risk for psychosis) program. *Am J Psychiatry* 2018;175:906–8.
- 19 Zhang T, Xu L, Tang Y, et al. Duration of untreated prodromal symptoms in a Chinese sample at a high risk for psychosis: demographic, clinical, and outcome. *Psychol Med* 2018;48:1274–81.
- 20 Jones SH, Thornicroft G, Coffey M, et al. A brief mental health outcome scale—reliability and validity of the global assessment of functioning (GAF). *Br J Psychiatry* 1995;166:654–9.
- 21 Smith SM, Jenkinson M, Johansen-Berg H, et al. Tract-based spatial statistics: voxelwise analysis of multi-subject diffusion data. *Neuroimage* 2006;31:1487–505.
- 22 Smith SM, Jenkinson M, Woolrich MW, et al. Advances in functional and structural Mr image analysis and implementation as fsf. *Neuroimage* 2004;23 Suppl 1:S208–19.
- 23 Nägele FL, Pasternak O, Bitzan LV, et al. Cellular and extracellular white matter alterations indicate conversion to psychosis among individuals at clinical high-risk for psychosis. *World J Biol Psychiatry* 2021;22:214–27.
- 24 Krakauer K, Ebdrup BH, Glenthøj BY, et al. Patterns of white matter microstructure in individuals at ultra-high-risk for psychosis: associations to level of functioning and clinical symptoms. *Psychol Med* 2017;47:2689–707.
- 25 Khan MM, Evans DR, Gunna V, et al. Reduced erythrocyte membrane essential fatty acids and increased lipid peroxides in schizophrenia at the never-medicated first-episode of psychosis and after years of treatment with antipsychotics. *Schizophr Res* 2002;58:1–10.
- 26 Reddy RD, Keshavan MS, Yao JK. Reduced red blood cell membrane essential polyunsaturated fatty acids in first episode schizophrenia at neuroleptic-naïve baseline. *Schizophr Bull* 2004;30:901–11.
- 27 Amminger GP, Schäfer MR, Klier CM, et al. Decreased nervonic acid levels in erythrocyte membranes predict psychosis in help-seeking ultra-high-risk individuals. *Mol Psychiatry* 2012;17:1150–2.
- 28 Rapoport SI. In vivo approaches to quantifying and imaging brain arachidonic and docosahexaenoic acid metabolism. *J Pediatr* 2003;143:26–34.
- 29 Keshavan MS, Stanley JA, Montrose DM, et al. Prefrontal membrane phospholipid metabolism of child and adolescent offspring at risk for schizophrenia or schizoaffective disorder: an in vivo 31P MRS study. *Mol Psychiatry* 2003;8:251:316–23.
- 30 Al Awam K, Haubleiter IS, Dudley E, et al. Multiplatform metabolome and proteome profiling identifies serum metabolite and protein signatures as prospective biomarkers for schizophrenia. *J Neural Transm* 2015;122 Suppl 1:111–22.
- 31 McNamara RK, Szeszko PR, Smesny S, et al. Polyunsaturated fatty acid biostatus, phospholipase A₂ activity and brain white matter microstructure across adolescence. *Neuroscience* 2017;343:423–33.
- 32 Devoe DJ, Braun A, Seredynski T, et al. Negative symptoms and functioning in youth at risk of psychosis: a systematic review and meta-analysis. *Harv Rev Psychiatry* 2020;28:341–55.



Wenjun Su is a PhD candidate at the Shanghai Jiao Tong University School of Medicine. She has been studying in the Department of EEG and Neuroimaging at Shanghai Mental Health Center, with an expectation to get her Doctor of Medicine degree in June 2022. Her research mainly focuses on utilizing multi-modal advanced neuroimaging techniques to understand the neural basis and the pathophysiological changes in psychosis. Her main research interests include revealing the anatomical and functional brain changes behind the complex psychotic symptoms of early-onset psychosis, which could potentially be further validated as biomarkers and lead to the development of identification and targeted treatment for psychosis.

Table S1. Tract-based spatial statistics (TBSS) analysis of fractional anisotropy (FA) in CHR group and HC group.

Cluster Index	1-p value	MNI coordinates			White matter tracts
		x	y	z	
FA CHR<HC	0.998	-14	25	19	Genu, Body, Splenium of corpus callosum Sagittal stratum (include inferior longitudinal Fasciculus and inferior fronto-occipital fasciculus) R L Anterior, Posterior limb of internal capsule R L Anterior, Superior, Posterior of corona radiata R L Cerebral peduncle R L External capsule R L Cingulum (Cingulate Gyrus) R Retrolenticular part of internal capsule R L Fornix (cres) / Stria terminalis R L Posterior thalamic radiation (include optic radiation) R L Medial lemniscus R L Fornix (column and body of fornix) Superior longitudinal fasciculus R L
RD CHR>HC	0.988	-14	25	19	Genu, Body, Splenium of corpus callosum Anterior, Posterior limb of internal capsule R L Anterior, Superior, Posterior of corona radiata R L Sagittal stratum (include inferior longitudinal Fasciculus and inferior fronto-occipital fasciculus) R L Superior longitudinal fasciculus R L Cerebral peduncle R L Superior cerebellar peduncle R L Inferior cerebellar peduncle L Middle cerebellar peduncle External capsule R L Cingulum (Cingulate Gyrus) R Posterior thalamic radiation (include optic radiation) R L Retrolenticular part of internal capsule R L Medial lemniscus R L Fornix (column and body of fornix) Fornix (cres) / Stria terminalis R L Superior fronto-occipital fasciculus R Pontine crossing tract (a part of MCP)
MD CHR>HC	0.993	-36	-56	21	Genu, Body, Splenium of corpus callosum Anterior, Posterior limb of internal capsule R Anterior, Superior, Posterior of corona radiata R L Superior longitudinal fasciculus R L Cerebral peduncle R L External capsule R L Posterior thalamic radiation (include optic radiation) R L

Sagittal stratum (include inferior longitudinal
Fasciculus and inferior fronto-occipital fasciculus) R
L
Retrolenticular part of internal capsule R L
Cingulum (Cingulate Gyrus) R
Fornix (cres) / Stria terminalis R
